The Astrophysical Journal, 785:56 (5pp), 2014 April 10 doi:10.1088/0004-637X/785/1/56

COMPLEXITY AND DIFFUSION OF MAGNETIC FLUX SURFACES IN ANISOTROPIC TURBULENCE

S. Servidio[1], W. H. Matthaeus[2], M. Wan[2], D. Ruffolo[3,4], A. F. Rappazzo[2,5], and S. Oughton[6]
[1] Dipartimento di Fisica, Università della Calabria, I-87036 Cosenza, Italy; sergio.servidio@fis.unical.it
[2] Department of Physics and Astronomy, University of Delaware, Newark, DE, USA
[3] Department of Physics, Faculty of Science, Mahidol University, Bangkok, Thailand
[4] Thailand Center of Excellence in Physics, CHE, Ministry of Education, Bangkok, Thailand
[5] Advanced Heliophysics, 127 East Del Mar Boulevard, Suite 425, Pasadena, CA 91106, USA
[6] Department of Mathematics, University of Waikato, Hamilton, New Zealand
Received 2013 December 1; accepted 2014 February 25; published 2014 March 25

ABSTRACT

The complexity of magnetic flux surfaces is investigated analytically and numerically in static homogeneous magnetic turbulence. Magnetic surfaces are computed to large distances in magnetic fields derived from a reduced magnetohydrodynamic model. The question addressed is whether one can define magnetic surfaces over large distances when turbulence is present. Using a flux surface spectral analysis, we show that magnetic surfaces become complex at small scales, experiencing an exponential thinning that is quantified here. The computation of a flux surface is of either exponential or nondeterministic polynomial complexity, which has the conceptual implication that global identification of magnetic flux surfaces and flux exchange, e.g., in magnetic reconnection, can be intractable in three dimensions. The coarse-grained large-scale magnetic flux experiences diffusive behavior. The link between the diffusion of the coarse-grained flux and field-line random walk is established explicitly through multiple scale analysis. The Kubo number controls both large and small scale limits. These results have consequences for interpreting processes such as magnetic reconnection and field-line diffusion in astrophysical plasmas.

Key words: ISM: magnetic fields – magnetic fields – magnetic reconnection – magnetohydrodynamics (MHD) – solar wind – Sun: magnetic fields

Online-only material: color figures

1. INTRODUCTION

Magnetic flux surfaces afford familiar descriptions of spatial structure, dynamics, and connectivity of magnetic fields, with particular relevance in contexts such as solar coronal flux tubes (Parker 1979; Kopp & Pneuman 1976; Wang & Sheeley 1990), magnetic field connectivity in the interplanetary and interstellar medium (Bruno et al. 2001; Borovsky 2008; Wright & Berger 1989; Crutcher 1991; Subramanian 1998; Zimbardo et al. 2004), and magnetic reconnection (Sweet 1958a, 1958b; Parker 1963; Petschek 1964), as well as in laboratory plasmas and dynamo problems (Rosenbluth et al. 1966; Zaslavskii & Chirikov 1972; Brandenburg & Subramanian 2005). Typical models assume that field lines are orderly and flux tubes remain identifiable over macroscopic distances; however, a previous study has shown that flux tubes shred in the presence of fluctuations, typically losing identity after several correlation scales (Matthaeus et al. 1995). Here, we quantify the growth of distortions of flux surfaces with increasing distance for a specific model, demonstrating both exponential scaling of the smallest features, and diffusive mixing at larger scales. These features mandate revision to models based on simple laminar flux tubes: it becomes exponentially more difficult to identify flux tubes over macroscopic distances. This has conceptual implications for magnetic reconnection theory and numerous astrophysical applications.

To frame the topic, we begin by pointing out related problems that are not addressed herein. First, we are not discussing either the dynamics of field lines, a notion that becomes poorly defined in the presence of nonideal effects including reconnection (Eyink et al. 2013), or the related problem of the time development of magnetic connectivity (Rappazzo et al. 2012). Second, we are not specifically concerned with the very short distance behavior of field lines and flux surfaces; in this regime one may find superdiffusive behavior akin to turbulent "Richardson diffusion," or exponential separation of trajectories at small separations (Zaslavskii & Chirikov 1972). Finally, we do not address similar concepts of relevance in laboratory plasmas, such as "good" and "destroyed" flux surfaces and Kolmogorov-Arnold-Moser (KAM) surfaces that emerge in a bounded volume with toroidal periodicity (Rosenbluth et al. 1966). The focus here is on statistically homogeneous nonperiodic astrophysical systems for which many elegant theorems that hold for the periodic toroidal case are not relevant.

Our concern is the magnetic field at a single instant of time in the presence of broadband turbulence as expected in astrophysical systems. By addressing the defining characteristic of flux tubes, this study addresses the underpinnings of numerous solar, heliospheric, and astrophysical applications. The topology of any magnetic field can be described in terms of magnetic surfaces, which are everywhere tangent to the field vector (Parker 1979). To construct these, begin with an arbitrary smooth closed contour C and a static magnetic field $\boldsymbol{B}(\boldsymbol{x})$. Transport every line element on C along the local direction of $\boldsymbol{B}$ to generate a surface S. Any topologically similar contour C' lying on S defines the edge of an open surface S'. Application of Gauss's law and $\nabla \cdot \boldsymbol{B} = 0$ shows that the magnetic flux $\Phi = \int_{S'} \widehat{\boldsymbol{n}} \cdot \boldsymbol{B}\, d^2x$ (where $\widehat{\boldsymbol{n}}$ is an oriented unit vector normal to S'), is the same for all S'. This defines the "flux tube" S, a surface tangent to the magnetic field, labeled by a value χ, which may be viewed as itself transported along the field. A family of flux tubes is defined by a nested set of coplanar contours $C(\chi)$, for a continuous flux label χ. These basic constructs describe flux tubes, flux ropes, magnetic connectivity, and magnetic topology.

The limit $\Phi \to 0$ produces a zero-volume flux tube, coinciding with a magnetic field line. Any flux function χ satisfies the flux surface differential equation $\boldsymbol{B} \cdot \nabla \chi = 0$, which forms the basis of our analysis below.

2. BACKGROUND AND NUMERICAL EXPERIMENT

To examine the spatial complexity of $\chi(x, y, z)$ in the presence of turbulence, we adopt a specific magnetic field model, $\boldsymbol{B} = \boldsymbol{B}_0 + \boldsymbol{b}$, where $\boldsymbol{B}_0 = B_0 \widehat{z}$ is a uniform mean field and $\boldsymbol{b}$ is the fluctuating component. Anisotropy associated with a strong mean magnetic field (Shebalin et al. 1983; Oughton et al. 1994; Bigot et al. 2008) is of substantial importance in space and astrophysics (Zank & Matthaeus 1992b; Bieber et al. 1994; Goldreich & Sridhar 1995). To capture this effect, we employ a reduced magnetohydrodynamic (RMHD) model (Strauss 1976; Montgomery 1982; Zank & Matthaeus 1992a), a nonlinear model valid when the normalized fluctuation amplitude $\delta b / B_0$ is a small parameter. Here, δb is the rms strength of the fluctuations $\boldsymbol{b}$. The total magnetic field is written as

$$\boldsymbol{B}(x, y, z) = B_0 \widehat{z} + \boldsymbol{\nabla}_\perp \times \widehat{z} a(x, y, z), \tag{1}$$

where $\boldsymbol{\nabla}_\perp = (\partial/\partial x, \partial/\partial y)$, and the magnetic potential a varies in three Cartesian directions, but only slowly with z. The RMHD model incorporates both variance anisotropy, i.e., $\boldsymbol{b} \cdot \boldsymbol{B}_0 = 0$, and spectral (or correlation) anisotropy, in that $\partial/\partial x \sim \partial/\partial y \gg \partial/\partial z$. This magnetic field is weakly three dimensional (3D) and is sometimes classified as "Alfvénic turbulence," because the polarization is reminiscent of linear Alfvén waves, or "quasi-two-dimensional," because the wavevectors are mostly within a small angle of the (x, y) plane.

For a uniform mean magnetic field with transverse fluctuations, the flux surface equation, $\boldsymbol{B} \cdot \nabla \chi = 0$, becomes

$$\frac{\partial \chi}{\partial z} + \frac{\boldsymbol{b}}{B_0} \cdot \nabla_\perp \chi = 0. \tag{2}$$

Equation (2) is of the same form as an ideal two-dimensional passive scalar equation (Matthaeus et al. 1995; Kadomtsev & Pogutse 1979), with correspondence of $\partial/\partial z$ with a (slow) time derivative, and of $\boldsymbol{b}/B_0$ with a two-dimensional incompressible velocity field. In analogy with passive tracers (Matthaeus et al. 1995), we expect flux surfaces to become increasingly "mixed" and complex with increasing z, even when the boundary data on χ, say at $z = 0$, are smooth. We now quantitatively describe this development of spatial complexity.

To analyze flux surfaces we specify $\boldsymbol{B}$ everywhere, choose a flux function $\chi(x, y, z = 0)$, and then solve Equation (2) for increasing z. To obtain $\boldsymbol{b}$ we perform a series of direct numerical simulations of RMHD turbulence, with resolution 1024^3, extracting the data at the time of peak nonlinear activity (after $\approx$ one nonlinear time). Details on the code can be found in Oughton et al. (2004). The domain is $L_x = L_y = 2\pi L_0$, and $L_z = 9L_x$. The dimensional wavevectors may be written as $\boldsymbol{k} = (m_x/L_0, m_y/L_0, m_z/(9L_0))$ for integer triplets (m_x, m_y, m_z). Initial conditions consist of a random phased superposition of Fourier modes for the magnetic and velocity fields, in the (dimensionless) wavenumber band $4 \leqslant \sqrt{m_x^2 + m_y^2} \leqslant 150$ and $|m_z| \leqslant 25$. The total fluctuation level is $\delta b = 1$. The perpendicular and parallel correlation lengths for $\boldsymbol{b}$, computed as the integral of its correlation functions, are $\ell_\perp = 0.088\, L_0$ and $\ell_z = 0.615\, L_0$, respectively, where L_0 is a characteristic length. Note that the derivation of the RMHD dynamical equations requires that $B_0 \gg \delta b$, while the parallel and perpendicular derivatives are ordered such that $B_0(\partial/\partial z) \sim \mathbf{b} \cdot \nabla_\perp$. In code units, the lengths and mean magnetic field are rescaled consistent with the latter relation.

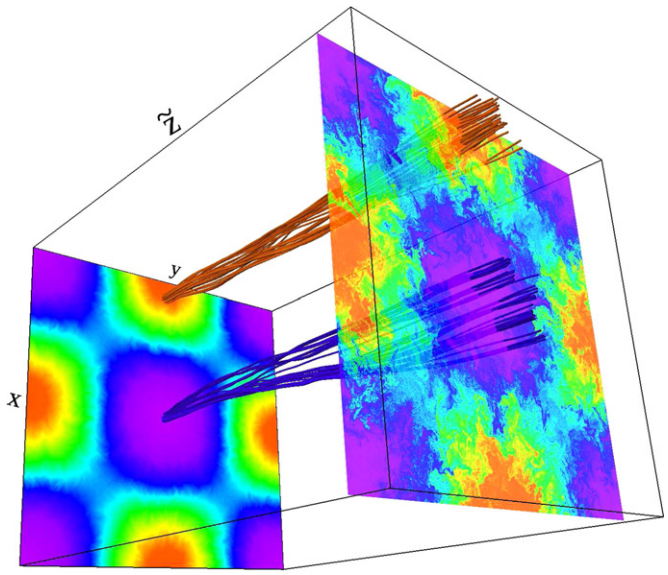

Figure 1. Flux function $\chi(x, y, z)$ at two distinct altitudes $\tilde{z} = z/\ell_z$, namely, $\tilde{z} = 0.4$ and 9.4. Two groups of field lines, starting from different topological regions, are also shown. Smooth initial flux tubes become complex, developing finer scales.

(A color version of this figure is available in the online journal.)

To solve Equation (2), we employ a separate fully de-aliased (2/3 rule) pseudospectral code, with fourth-order Runge–Kutta integration along z. Smooth boundary data are specified as $\chi(x, y, z = 0) \sim \cos x \cos y$, on a $N^2 = 1024^2$ Cartesian collocation grid.

In the diagnostics presented here, the value of B_0 is varied in order to explore different Kubo numbers:

$$R = \frac{\delta b}{B_0} \frac{\ell_z}{\ell_\perp}, \tag{3}$$

specifically cases with $R = 0.116$, 1.16, and 11.6.

It is well established that statistical transport properties of flux surfaces and field lines are regulated by the Kubo number (Kadomtsev & Pogutse 1979; Isichenko 1991). Organization of transport effects according to Kubo number has proven useful in various studies, for example, the small pitch angle cross field diffusion of cosmic rays (Hauff et al. 2010) and field-line separation effects on electron heat transport in coronal loops (Bitane et al. 2010). In the present context it is readily apparent from examination of Equation (2) that the Kubo number is the only parameter that enters in an RMHD description of flux surface transport (as well as the magnetic field-line random walk; see also Ruffolo & Matthaeus 2013).

Figure 1 shows cross-sections of the flux function for $R = 1.16$ at two distinct altitudes $\tilde{z}$, where $\tilde{z} = z/\ell_z$ is the normalized parallel coordinate. Tracing the magnetic surface(s) along $\tilde{z}$, a dramatic increase in complexity is observed. This effect was previously described as a qualitative context for development of nonlinear theories of magnetic field-line random walk (Matthaeus et al. 1995) and of perpendicular diffusion of charged particles (Matthaeus et al. 2003). Here, we will describe the phenomenon quantitatively, with refined techniques and more detailed analysis of the RMHD magnetic fields.

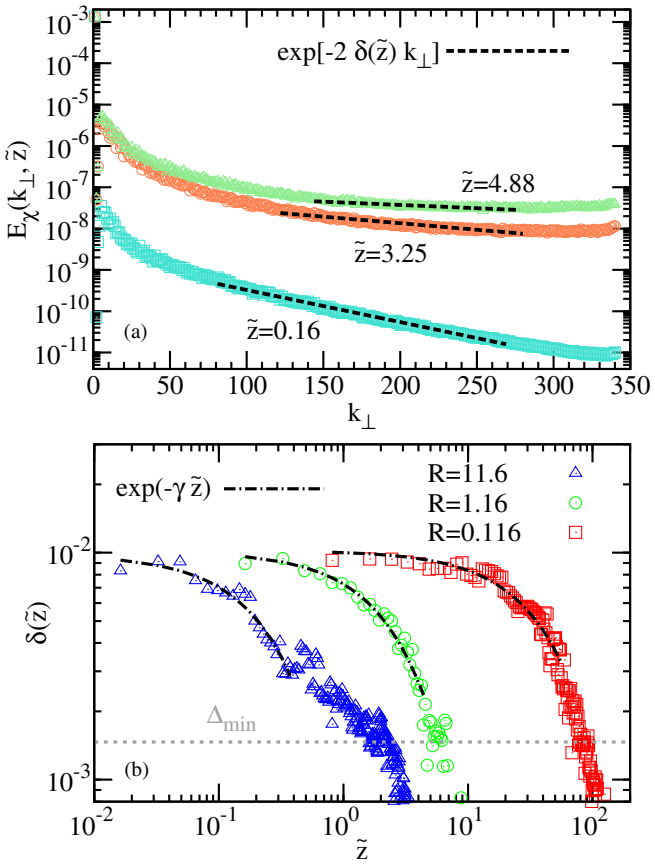

Figure 2. Top: spectrum E_χ of the magnetic flux function χ, for $R = 1.16$, at several $\tilde{z}$. An exponential fit is plotted with dashed (black) lines. Bottom: smallest excited scale of the system δ, as function of $\tilde{z}$, for several Kubo numbers R. An exponential fit is plotted with dot–dashed lines. The horizontal dashed (gray) line represents the Nyquist scale.

(A color version of this figure is available in the online journal.)

3. SMALL-SCALE ANALYSIS

Figure 1 shows that at larger $\tilde{z}$, a small amount of "thermalization" develops at small scales (Wan et al. 2009), associated with limited resolution. To quantify and control this effect, we introduce measures of numerical accuracy based on the exact conservation laws implied by Equation (2). A useful subset is the set of Casimir invariants $A^{\{n\}} = \int dx\, dy\ \chi^n(x, y, \tilde{z})$ with $n = 2, 4, 6, \ldots$, which are independent of $\tilde{z}$ according to Equation (2). Due to the accuracy of the spectral method, the fractional errors of these invariants are $\sim 10^{-8}$ when we carry out most analyses shown here, and $\sim 10^{-2}$ for the larger $\tilde{z}$ analyses shown.

To evaluate complexity in the magnetic flux function, it is useful to compute its power spectrum $E_\chi(k_\perp, \tilde{z}) = |\hat{\chi}(k_\perp, \tilde{z})|^2$, where $k_\perp = \sqrt{k_x^2 + k_y^2}$, and $\hat{\chi}$ is the Fourier decomposition of the flux function. Finer scale structures in χ produce higher wavenumber Fourier components. Figure 2(a) shows the χ spectra at several values of $\tilde{z}$, for the case with Kubo number $R = 1.16$. Emerging complexity is seen in the increased amplitudes at high wavenumber at larger $\tilde{z}$. To quantify this, at high $k_\perp$ we fit the χ spectra to an exponential

$$E_\chi(k_\perp, \tilde{z}) \sim e^{-2\delta(\tilde{z})k_\perp}, \tag{4}$$

thus defining a measure of the smallest excited scale $\delta(\tilde{z})$ (Frisch et al. 1983). As shown in Figure 2(a), the fit is confined to scales well-separated from both large (energy-containing) scales, and the smallest (thermalizing) scales.

Theoretical discussion based on an exponential form of the spectrum has been employed previously, in the study of current sheet thinning in ideal MHD (Frisch et al. 1983), and in the examination of possible finite time singularities in turbulence (Brachet et al. 1983, 2013; Sulem et al. 1983; Rappazzo & Parker 2013). The scale δ is interpreted as the distance in the complex plane to the nearest singularity. A systematic decrease of δ is suggestive of an approach to a real singularity (Brachet et al. 1983, 2013).

Here, we computed the decrease in $\delta(\tilde{z})$ with increasing $\tilde{z}$,

$$\delta(\tilde{z}) \sim e^{-\gamma\tilde{z}}, \tag{5}$$

and find approximately exponential behavior, with $\gamma > 0$, until accuracy becomes questionable at larger $\tilde{z}$. This is illustrated in Figure 2(b), which also shows the smallest physical resolved scale (Nyquist scale) $\Delta_{\min} = 1/(2k_{\max})$, where $k_{\max} = N/3$ is imposed by the de-aliasing procedure. The exponential fit in Equation (5) captures well the thinning of δ with increasing $\tilde{z}$. Evidently the Kubo number is the controlling parameter, and $\gamma = \gamma(R)$. For the cases shown, with $R = 0.116, 1.16, 11.6$, we obtained $\gamma \sim 0.02, 0.33, 3.3$ (in units of ℓ_z). We will return to this point later.

In principle, of course, use of greater spatial resolution might extend this range of exponential decrease. Adequate spatial resolution at large distances $\tilde{z}$ requires that a maximum wavenumber $k_{\max}$ be retained in the computation of χ such that $k_{\max}(\tilde{z})\delta(\tilde{z}) > 1$, or equivalently that the number of required Fourier modes scales as $N^2 \sim \exp(2\gamma\tilde{z})$. Note that the flux surface equation is fundamentally ideal, so there is no physical basis for adding small diffusivity to the rhs that would alleviate this requirement.

From the point of view of computability, unless a simplification is found, the problem of computation of flux surfaces would be placed in the class of exponential complexity, which describes formally intractable problems (Mertens 2002). Alternatively, it is possible that a simplified strategy might be found that allows the computation to be performed using a nondeterministic polynomial (or NP) approach, possibly requiring nonclassical computation (e.g., through exponential parallelism).

The difficulty in accurate computing of flux tubes over extended distances has conceptual implications. For example (Schindler et al. 1988; Yamada et al. 2010), there are two main approaches in defining the magnetic reconnection problem: one considers the global flux exchange between topologically distinct families of flux surfaces, indicated by the presence of an electric field along a separator that divides the families. Alternatively, reconnection may be defined locally, as the local breakdown of the ideal MHD frozen-in property. While the global definition may be criticized on other grounds (Schindler et al. 1988), our analysis suggests that the identification of families of flux surfaces—a requisite condition for the global definition, may be formally intractable in 3D. Therefore, the global characterization of reconnection may not always be realizable in a 3D turbulent magnetic field, as the distinct families of surfaces may extend beyond the limit of computability.

4. LARGE-SCALE ANALYSIS

At this point we establish a link between the large-scale complexity of flux surfaces and the theory of field-line random walk (Jokipii 1966; Jokipii & Parker 1968; Matthaeus et al.

1995; Shalchi & Kolly 2013; Ruffolo & Matthaeus 2013; Zimbardo et al. 2004), which is expressed in terms of individual magnetic field-line trajectories. It is useful to proceed using a multiple scale analysis (Frisch 1987; Biferale et al. 1995), in which the diffusion is expected at perpendicular scales $\ell^* \gg \ell_\perp$, which are large compared to the perpendicular correlation scale. Accordingly, we define $\epsilon = \ell_\perp/\ell^*$, and introduce slowly varying in-plane spatial scales $\boldsymbol{\eta} = (\eta_x, \eta_y)$ to complement the "fast" variation at scale $\boldsymbol{x} = (x, y)$, and similarly a slow scale ζ in the z direction to complement the fast variation of the coordinate z. Treating the coordinates as independent, we expand the flux function as $\chi(\boldsymbol{x}_\perp, z) \rightarrow \chi(\boldsymbol{x}, \boldsymbol{\eta}, z, \zeta) = \chi^{(0)} + \epsilon\chi^{(1)} + \epsilon^2\chi^{(2)} + \epsilon^3\chi^{(3)} + \ldots$, where all quantities may depend formally on $\boldsymbol{x}$, $\boldsymbol{\eta}$, z, and ζ. An averaging operator $\langle\cdots\rangle$ is introduced, such that for any F the mean (or coarse-grained) value $\langle F(\boldsymbol{x}, \boldsymbol{\eta}, z, \zeta)\rangle$ varies at the slow scales $\boldsymbol{\eta}$ and ζ only. Thus, for example, $\chi = \langle\chi\rangle + \chi'$ and the fluctuation χ' has a vanishing average value.

Treating slow and fast variables as independent (Nayfeh 1973), we substitute a diffusive ordering of parallel and perpendicular scales, $\nabla_\perp \rightarrow \nabla_x + \epsilon\nabla_\eta$ and $\nabla_z \rightarrow \partial_z + \epsilon^2\partial_\zeta$, into Equation (2) to obtain $\left(\partial_z + \epsilon^2\partial_\zeta\right)\chi + \boldsymbol{b}/B_0 \cdot \left(\nabla_x + \epsilon\nabla_\eta\right)\chi = 0$. Inserting the expansion of χ and equating to zero the sum of coefficients of like powers of ϵ, we find at $O(\epsilon^0)$ that $\partial_z\chi^{(0)\prime} + \boldsymbol{b}/B_0 \cdot \nabla_x\chi^{(0)\prime} = 0$. This is a linear homogeneous equation (lacking sources) and therefore, if at some plane (say $z = 0$) the leading-order flux surface function $\chi^{(0)}$ lacks small-scale structure, then $\chi^{(0)\prime}(z = 0) = 0$. This property will persist in z as long as the perturbation expansion remains valid. Consequently, we may specify that $\chi^{(0)\prime} = 0$.

At $O(\epsilon)$ we find the equation $\partial_z\chi^{(1)} + \boldsymbol{b}/B_0 \cdot \nabla_x\chi^{(1)} = -\boldsymbol{b}/B_0 \cdot \nabla_\eta\langle\chi^{(0)}\rangle$. The term on the right-hand side (rhs) acts as a source in the Lagrangian frame, and $\nabla_\eta\langle\chi^{(0)}\rangle$ is a constant relative to integration in the fast variable z. To solve, we integrate along Lagrangian characteristics to find $\chi^{(1)} = -\boldsymbol{q} \cdot \nabla_\eta\langle\chi^{(0)}\rangle + C$, where C is a constant of integration and $\boldsymbol{q} = \int_0^z dz'\, \boldsymbol{b}(\boldsymbol{x}(z'), z')/B_0$. Note that the quantity $\boldsymbol{q}$ is precisely the transverse displacement $\Delta\boldsymbol{x}(z)$ of a field line after traveling a distance z along $\boldsymbol{B}_0$, computed from solving the field-line equation $d\boldsymbol{x}(z)/dz = \boldsymbol{b}/B_0$. This reflects the fact that χ is constant along field lines.

The full $O(\epsilon^2)$ equation (not shown) contains some terms that are rapidly varying; their sum must be set to zero as a solvability condition. The remaining (slow) $O(\epsilon^2)$ terms imply that

$$\frac{\partial\langle\chi^{(0)}\rangle}{\partial\zeta} + \frac{\partial}{\partial\eta_i}\frac{\langle b_i\chi^{(1)}\rangle}{B_0} = 0. \quad (6)$$

Inserting the above solution for $\chi^{(1)}$, this becomes

$$\frac{\partial\langle\chi^{(0)}\rangle}{\partial\zeta} = \frac{\partial}{\partial\eta_i}\left[D^S_{ij}\frac{\partial\langle\chi^{(0)}\rangle}{\partial\eta_j}\right] \quad (7)$$

with

$$D^S_{ij} = \int_0^z dz' \frac{\langle b_i(\boldsymbol{x}(z), z)\, b_j(\boldsymbol{x}(z'), z')\rangle}{B_0^2}. \quad (8)$$

Equation (7) is a standard diffusion equation at slow (i.e., large) scales, as anticipated, while D^S_{ij} has the standard form of a Green–Kubo–Taylor diffusion tensor. Note that we may write the trace as $D_S = Tr(D^S_{ij}) = \langle\boldsymbol{b}(\boldsymbol{x}(z), z) \cdot \boldsymbol{q}(\boldsymbol{x}(z), z)\rangle/B_0 = \langle d\Delta\boldsymbol{x}(z)/dz \cdot \Delta\boldsymbol{x}(z)\rangle = (1/2)(d/dz)\langle|\Delta\boldsymbol{x}(z)|^2\rangle$. The last term is explicitly equivalent to the trace of the diffusion coefficient

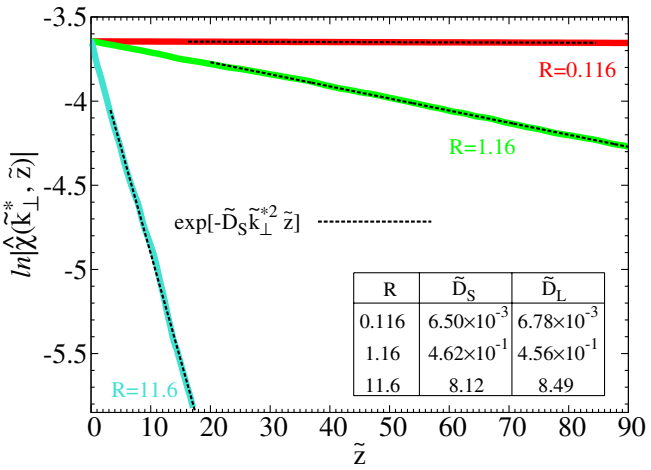

Figure 3. Large-scale Fourier mode of χ vs. $\tilde{z}$, for different R. The exponential fit (dashed black lines), consistent with Equation (9), determines the values $\tilde{D}_S$. In the table, $\tilde{D}_S$ are compared to the field-line diffusion coefficients $\tilde{D}_L$. Here, $\tilde{D}_{S,L} = D_{S,L}(\ell_z/\ell_\perp^2)$ are the normalized diffusion coefficients.
(A color version of this figure is available in the online journal.)

for a random walk of individual field lines, which we designate as D_L.

For axisymmetric turbulence transverse to z, in standard coordinates, we arrive at the diffusion problem

$$\frac{\partial\langle\chi\rangle}{\partial z} = D_S\nabla_\perp^2\langle\chi\rangle \quad (9)$$

for the coarse-grained flux surfaces $\langle\chi\rangle$. A numerical experiment is readily constructed to evaluate the flux surface diffusion coefficient D_S, which can be compared with the (formally equivalent) field-line diffusion coefficient D_L (computed from Lagrangian integration of an ensemble of 5000 magnetic field lines). The mean flux surface function $\langle\chi\rangle$ is conveniently defined as the large-scale band-limited boundary data at $\tilde{z} = 0$. Here, the wavenumber of the "initial" data for χ satisfies $\tilde{k}_\perp^\star = k_\perp^\star\ell_\perp = \ell_\perp/\ell^\star \ll 1$, as required. With increasing $\tilde{z}$, spectral excitation of χ spreads to higher $k_\perp$, as seen in Figure 2. Consequently, the initially excited Fourier modes "decay" and, according to Equation (9) one should find $|\hat{\chi}(\tilde{k}_\perp^\star, \tilde{z})| \sim \exp(-\tilde{k}_\perp^{\star 2}\tilde{D}_S\tilde{z})$. Figure 3 indicates that the large-scale mode $\hat{\chi}$ decays exponentially, as expected, for several Kubo numbers. From this exponential fit, values of D_S are obtained, and compared to the empirical field-line diffusion coefficients D_L. The table in Figure 3 shows good agreement between the two approaches, with the greatest error at ∼4%.

5. CONCLUSIONS AND DISCUSSION

In conclusion, we have quantified the complexity of magnetic flux surfaces computed at a single instant of time in anisotropic reduced MHD. The stretching of flux surfaces generates small-scale structure, and the perpendicular wavenumber spectrum of the flux function is well fit by an exponential $\sim\exp[-2\delta(z)k_\perp]$ in $k_\perp$ (see Equation (4)), in which the scale $\delta(z)$ is empirically determined to itself decrease approximately as an exponential: $\delta(z) \sim \exp[-\gamma(R)z]$. Our results suggest that the thinning distance $1/\gamma$ is ∼ the parallel correlation scale when the Kubo number ∼1 (consistent with Matthaeus et al. 1995). With this scaling, flux surfaces may become complex over scales $\sim 10^{-2}$ AU in the solar wind, and ∼35,000 km in the corona (Zimbardo et al. 2004). Under these conditions, accurate

computation of flux surfaces falls into a very difficult class (at best, NP) of problems.

It is tempting to associate the exponential thinning of flux surfaces observed here with local stochastic instability (Zaslavskii & Chirikov 1972; Isichenko 1992). However, in our numerical experiments, the exponential thinning of the smallest flux structures occurs (see Figures 2 and 3) in the same ranges of distance as does the diffusive behavior of the large-scale flux function. Thus field-line wandering, and presumably field-line separation, is algebraic, and not exponential. The often-encountered suggestion of "exponential separation of field lines" apparently is not occurring here. This notion has also been questioned previously for multi-scale magnetic turbulence (Ruffolo et al. 2004; Ragot 2008) such as is employed here. In these cases the linearization associated with computation of Lyapunov exponents is likely not applicable (e.g., Klyatskin 2008) at any but the shortest distances. A possible reconciliation of these ideas might be found in a reconsideration of the spread of magnetic flux, as illustrated, for example, in the "area mapping" cartoon of Rechester & Rosenbluth (1978). As the distribution becomes more complex, the shortest distance between any two fixed points (field lines) on the distribution may increase algebraically. However, the distance between the same two points measured along the distribution of flux may increase exponentially, as the flux structures stretch exponentially.

We have also shown how the ideal, nondissipative problem of flux surface transport is transformed into a diffusion problem by coarse-graining and utilizing methods of multiple scale analysis. The Eulerian approach given by coarse-grained magnetic flux is in good agreement with the Lagrangian field-line diffusion coefficient, providing a novel approach to the study of magnetic complexity. Moreover, both large-scale diffusion and small-scale thinning appear to be controlled by the Kubo number. These results have consequences for understanding and interpreting processes with wide-ranging astrophysical implications such as magnetic reconnection, field-line diffusion, and particle transport in solar, heliospheric, and galactic plasmas. Extensions to related time dependent problems (Rappazzo et al. 2012; Eyink et al. 2013), will be deferred to future work.

We acknowledge support by the project "POR Calabria FSE 2007/2013," Marie Curie Project FP7 PIRSES-2010-269297 "Turboplasmas," the USA NSF (AGS-1063439 and SHINE AGS-1156094), NASA (Heliophysics Theory NNX08AI47G and NNX11AJ44G), the Solar Probe Plus Project (ISIS Theory team), the MMS theory and modeling team, and the Thailand Research Fund. We acknowledge V. Carbone, P. Veltri, and Liya Wan for useful contributions.

REFERENCES

Bieber, J. W., Matthaeus, W. H., Smith, C. W., et al. 1994, ApJ, 420, 294
Biferale, L., Crisanti, A., Vergassola, M., & Vulpiani, A. 1995, PhFl, 7, 2725
Bigot, B., Galtier, S., & Politano, H. 2008, PhRvE, 78, 066301
Bitane, R., Zimbardo, G., & Veltri, P. 2010, ApJ, 719, 1912
Borovsky, J. E. 2008, JGR, 113, 8110
Brachet, M. E., Bustamante, M. D., Krstulovic, G., et al. 2013, PhRvE, 87, 013110
Brachet, M. E., Meiron, D. I., Orszag, S. A., et al. 1983, JFM, 130, 411
Brandenburg, A., & Subramanian, K. 2005, PhR, 417, 1
Bruno, R., Carbone, V., Veltri, P., Pietropaolo, E., & Bavassano, B. 2001, P&SS, 49, 1201
Crutcher, R. M. 1991, ApJ, 520, 706
Eyink, G., Vishniac, E., Lalescu, C., et al. 2013, Natur, 497, 466
Frisch, U. 1987, in Turbulenceed, ed. J. R. Herring & J. C. McWilliams (Lecture Notes from the NCAR-GTP Summer School; Singapore: World Scientific)
Frisch, U., Pouquet, A., Sulem, P.-L., & Meneguzzi, M. 1983, JMecT, 2, 191
Goldreich, P., & Sridhar, S. 1995, ApJ, 438, 763
Hauff, T., Jenko, F., Shalchi, A., & Schlickeiser, R. 2010, ApJ, 711, 997
Isichenko, M. 1992, RvMP, 64, 961
Isichenko, M. B. 1991, PPCF, 33, 809
Jokipii, J. R. 1966, ApJ, 146, 480
Jokipii, J. R., & Parker, E. N. 1968, PhRvL, 21, 44
Kadomtsev, B., & Pogutse, O. P. 1979, PPCF, 1, 649
Klyatskin, V. I. 2008, PhU, 51, 395
Kopp, R. A., & Pneuman, G. W. 1976, SoPh, 50, 85
Matthaeus, W. H., Gray, P. C., Pontius, D. H., Jr., & Bieber, J. W. 1995, PhRvL, 75, 2136
Matthaeus, W. H., Qin, G., Bieber, J. W., & Zank, G. P. 2003, ApJL, 590, L53
Mertens, S. 2002, CSE, 4, 31
Montgomery, D. C. 1982, PhS, T2/1, 83
Nayfeh, A. H. 1973, Perturbation Methods (New York: Wiley)
Oughton, S., Dmitruk, P., & Matthaeus, W. H. 2004, PhPl, 11, 2214
Oughton, S., Priest, E. R., & Matthaeus, W. H. 1994, JFM, 280, 95
Parker, E. N. 1963, ApJS, 8, 177
Parker, E. N. 1979, Cosmical Magnetic Fields (New York: Oxford Univ. Press)
Petschek, H. E. 1964, in The Physics of Solar Flares, ed. W. N. Hess (NASA SP-50; Washington, DC: NASA), 425
Rappazzo, A. F., Matthaeus, W. H., Ruffolo, D., Servidio, S., & Velli, M. 2012, ApJL, 758, L14
Rappazzo, A. F., & Parker, E. N. 2013, ApJL, 773, L2
Ragot, B. R. 2008, ApJ, 682, 1416
Rosenbluth, M. N., Sagdeev, R. Z., Taylor, J. B., & Zaslavski, G. M. 1966, NucFu, 6, 297
Rechester, A. B., & Rosenbluth, M. N. 1978, PhRvL, 40, 38
Ruffolo, D., & Matthaeus, W. H. 2013, PhPl, 20, 012308
Ruffolo, D., Matthaeus, W. H., & Chuychai, P. 2004, ApJ, 614, 420
Schindler, K., Hesse, M., & Birn, J. 1988, JGR, 93, 5547
Shalchi, A., & Kolly, A. 2013, MNRAS, 431, 1923
Shebalin, J. V., Matthaeus, W. H., & Montgomery, D. C. 1983, JPlPh, 29, 525
Strauss, H. R. 1976, PhFl, 19, 134
Subramanian, K. 1998, MNRAS, 294, 718
Sulem, C., Sulem, P.-L., & Frisch, U. 1983, JCoPh, 50, 138
Sweet, P. A. 1958a, in IAU Symp. No. 6, Electromagnetic Phenomena in Cosmical Physics, ed. B. Lehnert (Cambridge: Cambridge Univ. Press), 123
Sweet, P. A. 1958b, Nuovo Cimento Suppl., 8, 188
Wan, M., Oughton, S., Servidio, S., & Matthaeus, W. H. 2009, PhPl, 16, 080703
Wang, Y.-M., & Sheeley, N. R., Jr. 1990, ApJ, 355, 726
Wright, A. N., & Berger, M. A. 1989, JGR, 94, 1295
Yamada, M., Kulsrud, R., & Ji, H. 2010, RvMP, 82, 603
Zank, G. P., & Matthaeus, W. H. 1992a, JPlPh, 48, 85
Zank, G. P., & Matthaeus, W. H. 1992b, JGR, 97, 17189
Zaslavskii, G. M., & Chirikov, B. V. 1972, SvPhU, 14, 549
Zimbardo, G., Pommois, P., & Veltri, P. 2004, JGR, 109, A02113